Stoichiometric Model and Flux Balance Analysis for a Mixed Culture of *Leptospirillum ferriphilum* and *Ferroplasma acidiphilum*

M. P. Merino, B. A. Andrews, and J. A. Asenjo
Dept. of Chemical Engineering and Biotechnology, Centre for Biotechnology and Bioengineering, CeBiB, University of Chile, Beauchef, 850 Santiago, Chile

DOI 10.1002/btpr.2028
Published online December 23, 2014 in Wiley Online Library (wileyonlinelibrary.com)

The oxidation process of sulfide minerals in natural environments is achieved by microbial communities from the Archaea and Bacteria domains. A metabolic reconstruction of two dominant species, Leptospirillum ferriphilum *and* Ferroplasma acidiphilum*, which are always found together as a mixed culture in this natural environments, was made. The metabolic model, composed of 152 internal reactions and 29 transport reactions, describes the main interactions between these species, assuming that both use ferrous iron as energy source, and* F. acidiphilum *takes advantage of the organic compounds secreted by* L. ferriphilum *for chemomixotrophic growth. A first metabolic model for a mixed culture used in bacterial leaching is proposed in this article, which pretends to represent the characteristics of the mixed culture in a simplified manner. It was evaluated with experimental data through flux balance analysis (FBA) using as objective function the maximization of biomass. The growth yields on ferrous iron obtained for each microorganism are consistent with experimental data, and the flux distribution obtained allows understanding of the metabolic capabilities of both microorganisms growing together in a bioleaching process. The model was used to simulate the growth of* F. acidiphilum *on different substrates, to determine* in silico *which compounds maximize cell growth, and which are essential. Knockout simulations were carried out for* L. ferriphilum *and* F. acidiphilum *metabolic models, predicting key enzymes of central metabolism. The results of this analysis are consistent with experimental data from literature, showing a robust behavior of the metabolic model.* © 2014 American Institute of Chemical Engineers *Biotechnol. Prog.*, 31:307–315, 2015
Keywords: bioleaching, mixed culture, Leptospirillum ferrooxidans*,* Ferroplasma acidiphilum*, iron oxidizing bacteria, archaea, flux balance analysis, stoichiometric model*

Introduction

Bioleaching is the oxidation process of metallic sulfide to soluble metallic ions and sulfuric acid, catalyzed by microorganism consortia.[1] Possibly, the main role of these microorganisms in bioleaching operations is to oxidize iron and sulfur containing minerals.[2]

Oxidation of ore by consortia of microorganisms generally takes place at a higher rate than with pure cultures, however, the specific role of each microorganism in these natural environments remains unclear, as well as the factors that enable their growth in communities. Therefore, it is essential to identify the microorganisms that compose these consortia, study their interactions in bioleaching operations, and then predict and explore the metabolic details that control these communities.

Microorganisms involved in metal recovery from sulfide minerals include members of the Bacteria and Archaea domains. Species of *Leptospirillum* and *Ferroplasma* genus are the dominant members of microbial communities in acid mine drainage and bioleaching environments.[3–6]

Leptospirillum ferriphilum is an autotrophic, mesophilic, acidophilic, and iron oxidizing bacteria. It plays an important role in bioleaching processes given its ability to attach to sulfide mineral, its high affinity for ferrous iron, and its low sensitivity to inhibition by ferric iron.[7,8]

Ferroplasma acidiphilum is a recently described mesophilic, acidophilic, ferrous iron oxidizing, and cell wall-lacking archaea. Different strains of *F. acidiphilum* have been isolated and characterized.[9–13] These strains were classified by Dopson et al.[9] as chemoorganotrophic, because they are able to grow on yeast extract or another source of organic carbon as the only energy source, and also chemomixotrophic, because they are capable of growth on ferrous iron as electron donor, but require a small amount (0.02% wt/vol) of yeast extract which, in this case, is essential for growth.

The main objective of the reconstruction of metabolic pathways is determining the relationship between genome and physiology of a microorganism. Through metabolic reconstruction it is possible to break down the metabolic pathways of an organism into their respective reactions and enzymes, allowing analysis of them into a complete network context.

Information from fully sequenced genomes allows the strain specific global reconstruction of metabolic networks, permitting further structural and functional studies for a

Correspondence concerning this article should be addressed to J. A. Asenjo at juasenjo@ing.uchile.cl.

particular microorganism. These models have been proven to be an effective strategy to enhance physiological studies of environmentally relevant microorganisms and predict physiological responses of these microorganisms to environmental or genetic stimuli.[14]

Additionally, in mixed cultures the interactions between individual species should be addressed to understand the behavior of microbial communities through mathematical modeling.[15,16]

The whole metabolism of two bioleaching bacteria, *A. ferrooxidans*[17] and *L. ferrooxidans,*[18] were developed and evaluated through metabolic flux analysis (MFA) to predict their metabolic behavior. In this work, for the first time a metabolic model of a mixed culture of bioleaching microorganisms composed of *L. ferriphilum* and *F. acidiphilum* was developed, in order to define, in a simplified manner, the metabolic characteristics and molecular mechanisms underlying of these biomining species, and predict their behavior when they are growing in a mixed culture.

Materials and Methods

Metabolic reconstruction

A metabolic reconstruction of *L. ferriphilum* was developed based on a previous metabolic model of *L. ferrooxidans*.[18]

The metabolic model of *F. acidiphilum* was built considering the main metabolic pathways of this archaea described in literature. Also, the reconstruction was based on the analogs archaea *Ferroplasma acidarmanus* Fer1 genome annotation, which is available in the Doe Joint Genome Institute website (JGI, http://www.jgi.doe.gov/genome-projects/).

Flux balance analysis

Flux balance analysis (FBA) was carried out as described previously.[18]

The metabolic model was implemented in the software Insilico Discovery 3.2 (Stuttgart, Germany, www.insilico-biotechnology.com).

Results and Discussion

Metabolic reconstruction of L. ferriphilum

The model of *L. ferriphilum* was modified in a few aspects with respect to the *L. ferrooxidans* model of Merino et al.[18] The TCA cycle was included in a reductive manner[19] for CO_2 assimilation, therefore the reductive acetyl-CoA pathway was not included. Ammonia fixation was considered to occur through the GDH pathway. In addition, exopolysaccharide (EPS) formation by the Leloir pathway was incorporated into the metabolic model.[20]

Canonical pathways (other fueling reactions, synthesis of precursor metabolites, biosynthesis of building blocks, and macromolecules biosynthesis) were considered to be analogous in both types of *Leptospirillum*.

Metabolic reconstruction of F. acidiphilum

Fueling Reactions. ***Glycolysis.*** According to Dopson et al.[21] *F. acidiphilum* growing in chemomixotrophic conditions up-regulates the enzymes fructose 1.6-bisphosphatase and phosphoglycerate mutase, so it is assumed that the conversion of glucose to pyruvate occurs via the Embden-Meyerhof-Parnas (EMP) pathway (reactions 1–6 in Appendix 1)

Pentose phosphate pathway (PPP). All autotrophic and heterotrophic archaea must be able to generate NAD(P)H and pentoses as building blocks for the biosynthesis of nucleotides and certain amino acids, so oxidative and nonoxidative branches of PPP were included in the stoichiometric model (reactions 7–12).

TCA cycle. All the enzymes of the TCA cycle were identified in the genome annotation of *Ferroplasma acidarmanus* Fer1, and then included in the stoichiometric model (reactions 13–19).

Anaplerotic reactions. To regenerate oxaloacetate, anaplerotic reactions catalyzed by pyruvate carboxylase and phosphoenolpyruvate carboxylase were included in the stoichiometric model. For simplicity, other anaplerotic reactions, such as the glyoxylate shunt, have not been included (reactions 20 and 21).

Oxidative phosphorylation. The electron transport chain involved in iron oxidation was approximated to the one of *F. acidarmanus* Fer1 for chemomixotrophic growth, which contains a putative haeme-copper terminal oxidase, cytochrome b, and associated Rieske iron-sulfur proteins, and a blue copper protein.[21] The net reaction of electron transport from Fe^{2+} is the following:

$$2Fe^{2+} + 1/2O_2 + 2H^+ \rightarrow 2Fe^{3+} + H_2O \quad (1)$$

The electrons derived from organic compound oxidation feed both an NADH ubiquinone oxidoreductase complex to generate reducing power, and a succinate dehydrogenase to oxidize succinate to fumarate, and transfer the electrons to a coenzyme Q, which is reduced to a coenzyme QH_2. Then, the electrons are carried to the rest of the previously mentioned transport chain. Also, the NADH ubiquinone oxidoreductase pumps protons to the external space as it transfers the electrons to the transport chain. The amount of pumped protons to the periplasmic space was taken from the proposed transport chain for *Ferroplasma acidarmanus* Fer1 available on http://www.microbesonline.org/. These reactions are summarized as follow:

$$NAD^+ + 4H^+_{INT} + coQ + H^+ \rightarrow NADH + 4H^+_{EXT} + coQH_2 \quad (2)$$

$$SUC + coQ \rightarrow FUM + coQH_2 \quad (3)$$

On the other hand, it was assumed that *Ferroplasma acidiphilum* produces ATP by an ATP synthetase coupled to the transport of 3 H^+.

$$3H^+_{EXT} + ADP + Pi + H^+ \rightarrow ATP + 3H^+_{INT} + H_2O \quad (4)$$

Biosynthetic reactions

Amino Acids Biosynthesis. The pathways for the synthesis of 20 standard amino acids were included in the stoichiometric model. The enzymes involved in each pathway were verified in the genomic annotation of *Ferroplasma acidarmanus* Fer1. Amino acids and their main precursors are shown in reactions 25–50.

Nucleotide Biosynthesis. Nucleotides in the form of ribonucleotides and deoxyribonucleotides were included as building blocks for RNA and DNA. All nucleotides were expressed as monophosphates, assuming that their activation

to triphosphates is carried out by polymerization reactions to RNA and DNA (reactions 51–59).

Archeal Phospholipid Biosynthesis. Membrane lipids in Archaea are composed of ether lipids containing saturated isopranyl chains, archaeol, and caldarchaeol.[22] The lipid composition of *F. acidiphilum* includes two main glycophospholipids, which comprise 90% of the total lipids. These main components are β-D-glucopyranosylcaldarchaetidylglycerol and a triglycoside of caldarchaetidylglycerol[12,23]; both components were included in the model as the only lipids in *F. acidiphilum*. The common precursor of these lipids is archaetidylglycerol, which was included as the only phospholipid in the model.

The biosynthetic pathway of archaetidylglycerol begins with the synthesis of the G-1-P backbone, which is formed from dihydroxyacetonephosphate (DHAP) by the enzyme G-1-P dehydrogenase.[24] In the model, DHAP was replaced by its isomer GAP (glyceraldehyde 3-phosphate), giving the formation reaction 60 in Appendix 1.

On the other hand, the isoprenoid biosynthetic pathway starts from acetyl-CoA to isopentenyl diphosphate (IPP) and dimethylallyl diphosphate (DMAPP) through the classical mevalonate (MVA) pathway, which has been identified in archaea.[22,25] DMAPP is condensed consecutively with several IPP molecules resulting in the synthesis of polyprenyl diphosphate compounds. For the model the formation of the 20 carbon geranylgeranyl diphosphate (GGPP) molecule was considered as the precursor of archeatidylglycerol. Furthermore, GGPP molecules were expressed as a function of IPP molecules as shown in reaction 61. GGPP is transformed to CDP-archaeol through the consecutive action of GGGP, DGGGP (archaetidic acid), and CDP-archaeol synthases, which is finally converted to archaetidylglycerol by archaetidylglycerophosphate synthase and phosphatase.[25]

Synthesis of macromolecules

Protein Biosynthesis. Protein amino acid composition of *F. acidiphilum* was approximated with an average composition obtained from the proteomic analysis of different species of archaea.[26] Protein biosynthesis requires 4.3 ATPs for the correct addition of one amino acid to the existing polypeptide[27] (reaction 64, Appendix 1).

DNA Biosynthesis. The G+C chromosomal composition of *F. acidiphilum* is ~35%,[12] so a composition of dGMP + dCMP of 35% and dAMP + dTMP of 65% per base pair was assumed. A consumption of 6.8 ATPs was calculated as the energy requirement for 1 bp formation of DNA (reaction 65). This value takes into account the ATP necessary for nucleotide incorporation, the separation of the double helix, the activation of monophosphates to triphosphates, and the energetic cost of proofreading.[27]

RNA Biosynthesis. From the DNA composition, the GMP + CMP nucleotide composition was approximated to 0.175% and 0.325% for AMP + UMP. An energetic cost of 2.4 ATPs was assumed for the synthesis of one nucleotide of RNA, 2 from the activation of monophosphates to triphosphates and 0.4 for the incorporation of one ribonucleotide[28] (reaction 66).

Lipid Biosynthesis. Two glycophospholipids are formed from archaetidylglicerol (β-D-glucopyranosylcaldarchaetidylglycerol and a triglycoside of caldarchaetidylglycerol, named lipI and lipII in reactions 67–69), comprising 90% of the total lipids.[12]

Carbohydrate Biosynthesis. Carbohydrates for cell wall biosynthesis, energy storing molecules and metabolites were defined as molecules $C_n(H_2O)_m$, and arise from the polymerization of glucose-6-phosphate (reaction 70).

Biomass Formation. Biomass relative composition of Protein, RNA, DNA, lipids, and carbohydrates were estimated for an average prokaryotic cell, obtaining 63% protein, 24% RNA, 4% DNA, 5% lipids, carbohydrates less than 1% and 4% of soluble pools.[29]

Simplification Criterion. As mentioned before, one of the objectives of this work is obtaining a simple but meaningful metabolic model. Therefore, the stoichiometric models were subjected to a general reduction process of matrix *S* based on a simplification criterion according to Stephanopoulos,[27] as follows:

i. Sequential reactions were lumped into a single reaction to reduce the number of reaction steps without affecting the resulting fluxes. These reactions are assumed to be at steady state, as well as the metabolites participating in them. This is the case of the intermediate metabolites that have only one route of generation and one route of consumption, for example intermediate metabolites for amino acids biosynthesis.
ii. ATP and ADP were considered the only energy transporters. Pyrophosphate was interpreted as two single phosphates.

Only NADH/NAD^+ were considered as cofactors for fueling and biosynthetic reactions, because the action of nicotidamide nucleotide transhydrogenase was supposed and NADH/NAD^+ are assumed to be equivalent to NADPH/$NADP^+$.

i. Metabolites that are freely interconvertible were represented as a single metabolite. For example DHAP and G3P were both represented as G3P in the models.
ii. The EPS formation flux by *L. ferriphilum* is equal to the EPS degradation flux by *F. acidiphilum* because it is assumed that the reactions are in steady state.
iii. EPS were expressed as glucose-6-phosphate in both models.

Flux Balance Analysis for a Mixed Culture. The underdetermined system of stoichiometric equations was solved using linear programming through FBA.[30]

A FBA was performed on the simple model of *L. ferriphilum*. The system of equations was solved in order to obtain the unknown fluxes by using as objective function the maximization of biomass. The constraints of the system were given by the steady state flux balances, from Eq. (1).

From the stoichiometric model, a standard composition of biomass of *L. ferriphilum* was determined as $CH_{1.9}O_{0.7}N_{0.2}P_{0.06}S_{0.002}$, therefore a molecular weight of 29 GDW per mole of carbon was calculated. This value is the biomass Yield coefficient per carbon, $Ycx = 29\left(\frac{GDW}{mole-C}\right)$.

Considering a specific growth rate of 0.081 (1/h),[31] the specific carbon uptake rate was calculated with the equation:

$$qCO2 = \frac{\mu}{Ycx}\left(\frac{mole}{GDW.h}\right) \quad (5)$$

Therefore, a specific consumption rate of CO_2, $qCO2 = 2.75$ (mmol/GDW/h) was used as input data for a

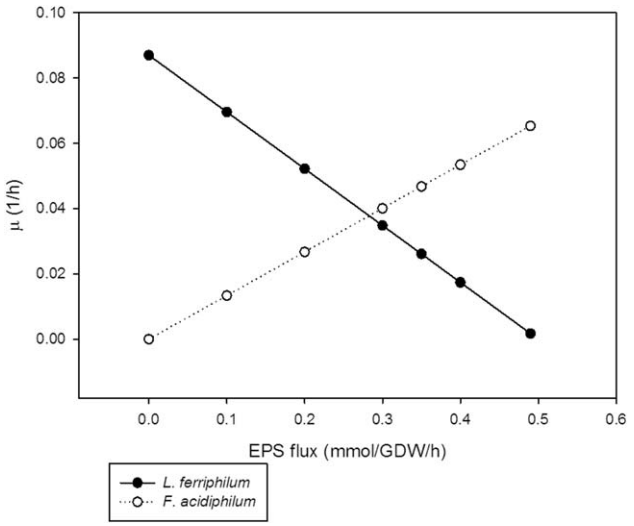

Figure 1. Sensitivity analysis of EPS flux formation on specific growth rates of *L. ferriphilum* and *F. acidiphilum*.

flux balance analysis of *L. ferriphilum*. This analysis showed that the maximization of biomass is achieved for a null flux of glucose through the Leloir pathway for EPS formation, which is very reasonable since this pathway results in a leak of carbon resources. Hence, the system was analyzed including the constraint of EPS formation flux, and also the sensibility of the objective function with respect to this constraint was studied. This analysis showed that for fluxes greater than 0.5 (mmol glucose/GDW/h) in the Leloir pathway, the system becomes unfeasible because it cannot be reached for the considered specific consumption rate of CO_2.

With the results of the sensitivity analysis, a FBA was executed for the mixed model of *L. ferriphilum* and *F.acidiphilum*, assuming that the latter consumes the EPS secreted by *L. ferriphilum*. The simulations were carried out using as input data the consumption rate of $qCO2 = 2.75$ (mmol CO_2/GDW/h) of *L. ferriphilum* and the different fluxes of EPS formation from the sensitivity analysis. In this case, the objective function was the maximization of biomass of both populations, and the constraints were specified by the steady state mass balances of each stoichiometric model. Under the specified aforementioned conditions, the variation of the specific growth rates of *L. ferriphilum* and *F. acidiphilum* related to the EPS flux are shown in Figure 1.

As expected, increasing the production flux of EPS in *L. ferriphilum* results in a decrease of its specific growth rate, because more carbon is directed to this purpose and not to biomass production. Likewise, the specific growth rate of *F. acidiphilum* increases with higher EPS flux, because it has more carbon source available.

A growth rate of 0.016 (h^{-1}) was assumed for *Ferroplasma acidiphilum* for chemomixotrophic growth.[12] With this data and Figure 1, an EPS flux distribution of $q_{EPS} = 0.127$ (mmol EPS/GDW/h) is obtained. Using this scenario, the metabolic fluxes for both networks were determined and the resulting fluxes are shown in Figure 2.[32,33]

With this flux distribution a biomass yield on ferrous iron was calculated for both populations, resulting in $Y_{FeX} = 0.0016$ (mol-C/mol Fe^{+2}) for *L. ferriphilum* and $Y_{FeX} = 0.037$ (mol-C/mol Fe^{+2}) for *F. acidiphilum,* which are very realistic values compared with yields obtained for *L. ferriphilum* ($Y_{FeX} = 0.002$ (mol-C/mol Fe^{+2}) by Gahan et al.[31] and for *F. acidiphilum* ($Y_{FeX} = 0.043$ (mol-C/mol Fe^{+2}), considering a composition of 62% of proteins) by Golyshina et al.[10]

The flux distribution is shown in Figure 2. Under the described conditions, the only active anaplerotic enzyme in *L. ferriphilum* and *F. acidiphilum* is phosphoenolpyruvate carboxylase, whereas pyruvate carboxylase turns out to be inactive for optimization purposes.

Little is known about archaeal enzymes involved in pentose conversion. Genes encoding canonical enzymes of the oxidative branch of the pentose phosphate pathway have not been identified in archaea.[34–36] In this simulation, the oxidative branch of the pentose phosphate pathway in *F. acidiphilum* is inactive. Therefore, it is proposed that the nonoxidative branch for pentose formation is fed from fructose 6-phosphate of the Embden–Meyerhof pathway by transketolase activity.[37]

Flux Balance Analysis of F. acidiphilum in Pure and Mixed Culture. Using as input data the specific consumption rates obtained in the previous simulation, the metabolic model of *F. acidiphilum* was used to simulate growth of this archaea on different substrates.

First, the effect of chemoautotrophic growth of *F. acidiphilum* on biomass generation by suppressing the EPS consumption flux on the model was explored, considering CO_2 assimilation through the reductive Acetyl-CoA pathway (Eq. (6)) and ferrous iron oxidation as energy source. In this scenario it was found that biomass formation is not possible, so input of an organic compound such as glucose as carbon source for *F. acidiphilum* is necessary, reaffirming a chemomixotrophic growth as described by Dopson et al.[9]

$$\text{Methyl}-\text{THF}+2\ \text{NADH}+\text{CO}_2+\text{CoA}+2\ \text{H}^+ \Rightarrow \text{Ac}-\text{CoA}+2\ \text{NAD}+\text{THF}+\text{H}_2\text{O} \quad (6)$$

It has been shown that *Ferroplasma acidiphilum* requires a small amount of yeast extract for growth. However, it is not clear which component of the yeast extract is being used as growth factor, remaining uncertain if it is a specific amino acid, vitamin, or the organic compounds from the yeast extract.

Simulations of growth on different substrates were tested in order to get a notion about the substrates from yeast extract that could be used for growth. For this, exchange reactions for specific amino acids and sugars were added to the metabolic model. The simulations were performed with FBA by maximization of *F. acidiphilum* biomass production rate as the objective function, and the maximum substrate uptake rate was set at an arbitrary value of 10 (mmol/GDW/h) for every substrate. The specific growth rates obtained in each simulation are shown in Table 1. All simulations were carried out considering an input flux of EPS, expressed as glucose, of 0.127 (mmol EPS/GDW/h), because it was observed that in the absence of this input, biomass generation is not possible.

It was assumed that the addition of cysteine or methionine as organic sulfur sources could increase the specific growth rate of *F. acidiphilum*; however, according to the estimations

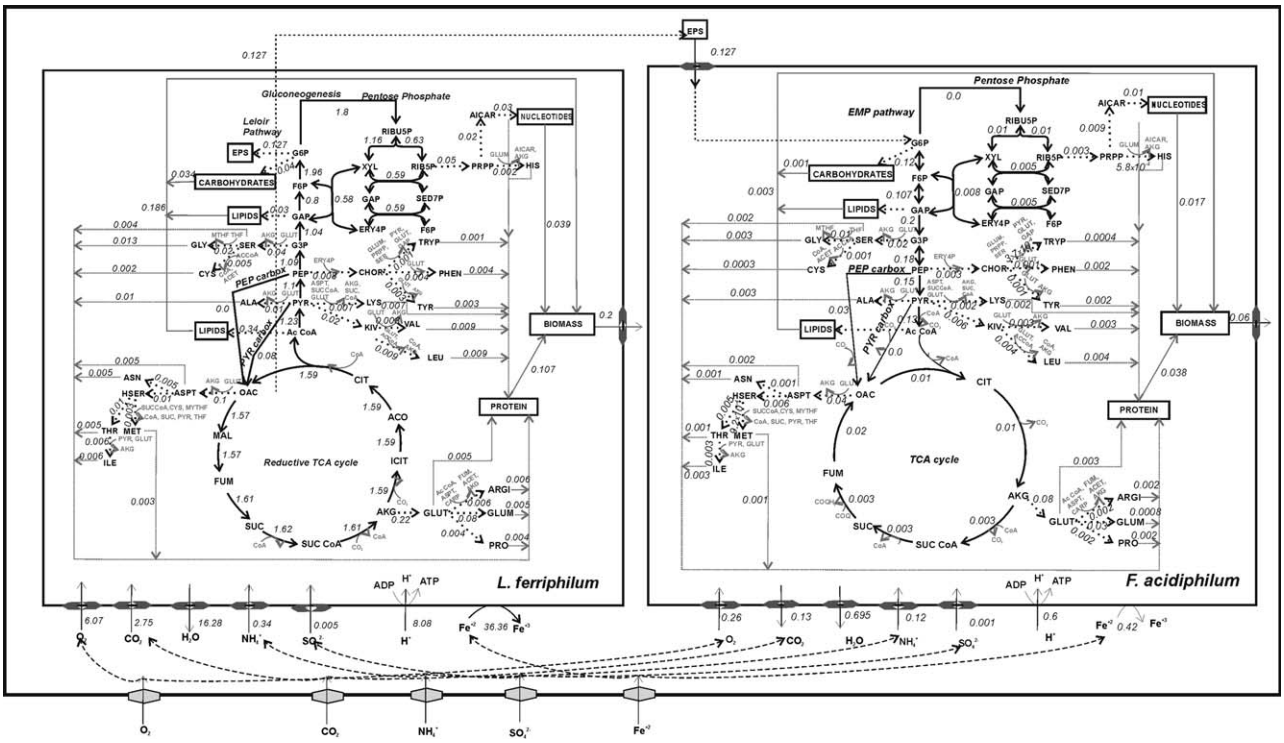

Figure 2. Flux distribution for a mixed culture of *L. ferriphilum* and *F. acidiphilum*.

Table 1. Specific Growth Rate of *F. acidiphilum* on Different Substrates Estimated by FBA

Substrate	Growth Rate (h^{-1})
Base	0.015
Glutamic acid	0.018
Glutamine	0.018
Cysteine	0.015
Asparagine	0.015
Aspartic acid	0.017
Methionine	0.015
Phenylalanine	0.015
Serine	0.537
Tyrosine	0.015
Valine	0.015

shown in Table 1, the addition of these amino acids, as well as asparagine, phenylalanine, valine, and tyrosine do not cause any increase in cell growth.

Other substrates such as glutamic acid, glutamine, and aspartic acid cause a slight rise in specific growth rate, because these amino acids are connected with the biosynthesis of important precursors of building blocks like oxaloacetate and α-ketoglutarate, and also aspartic acid is related to the biosynthetic pathways of nucleotides and other amino acids.

An important increase in specific growth rate is observed with serine, which is related to biosynthesis of purines and pyrimidines and with the synthesis of tryptophan, cysteine, and glycine. It is also involved in the metabolism of tetrahydrofolate, which acts as a coenzyme transporting carbon groups.

The exchange of metabolites between both species was explored. For this purpose, transport reactions of several amino acids (cysteine, glutamate, glutamine, asparagine, aspartate, methionine, phenylalanine, serine, tyrosine, and valine) were included in both stoichiometric models, and the exchange fluxes were unconstrained, so free fluxes of these amino acids between the microorganisms was tested by FBA. The specific growth rates obtained for the two species were 0.018 (h^{-1}) and 0.014 (h^{-1}) for *L. ferriphilum* and *F. acidiphilum* correspondingly.

Assuming that *F. acidiphilum* grows using the biological matter generated by *L. ferriphilum*, the amino acids exchange fluxes were tested only in one direction, secreted from *L. ferriphilum* and consumed by *F. acidiphilum*. In this case, the FBA predicts that the only amino acids that could be exchanged are glutamate, glutamine and serine, causing a slight increase in the growth rate of *F. acidiphilum* to 0.015 (h^{-1}) in the case of glutamate and glutamine, and 0.019 (h^{-1}) for serine, and a decrease in the specific growth rate of *L. ferriphilum* to 0.015 (h^{-1}) and 0.012 (h^{-1}), respectively. This assumption is made because *L. ferriphilum* is an autotrophic bacteria and *F. acidiphilum* is an heterotrophic archea. In lab tests, we observed that *L. ferriphilum* cannot grow in the presence of organic carbon sources, such as aminoacids, unlike *F. acidiphilum* that we proved empirically can grow in the presence of aminoacids, yeast extract, and other organic carbon sources. This assumption is necessary because of the information that we had about these microorganisms, in order to model the interactions between them. Also, in pure culture, in absence of a carbon source *F. acidiphilum* is unable to grow, but if it is mixed with *L. ferriphilum,* they can grow together using the organic matter secreted of *L. ferriphilum* (such as EPS).

Considering that we did not have the full genomic annotation for these organisms, and the uncertainty about the interactions of them growing in mixed culture, we considered for

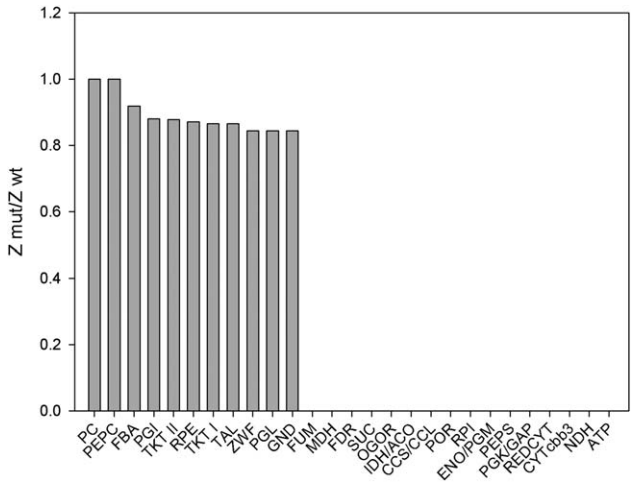

Figure 3. Enzyme knockouts in *L. ferriphilum* central metabolism obtained by FBA, using maximization of growth as objective function. Lumped reactions catalyzed for more than one enzyme were included with a slash (/).

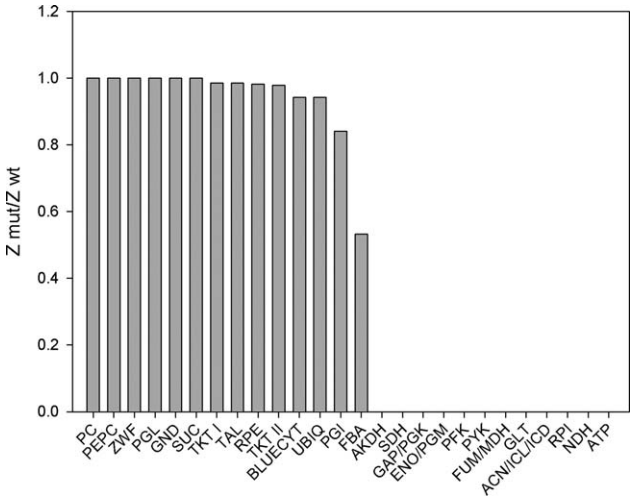

Figure 4. Enzyme knockouts in *F. acidiphilum* central metabolism obtained by FBA, using maximization of growth as objective function. Lumped reactions catalyzed for more than one enzyme were included with a slash (/).

the development of the mixed model some experimental information that was available to supply the lack of genomic information, in order to make a representative model of the system, and not a general model.

Knockout Simulations. To simulate enzyme knockouts, the associated reaction to the enzyme was constrained by setting the upper and lower bounds of the reaction to 0 (mmol/GDW/h). The enzyme knockouts tested corresponded to main enzymes involved in central metabolic pathways such as glycolysis/gluconeogenesis, pentose phosphate pathway and TCA (or reductive TCA cycle for *L. ferriphilum*), anaplerotic reactions, and respiration.

Knockout simulations were carried out for each model with FBA methodology, using as input data the consumption rates of carbon and energy sources (q_{CO2} and q_{Fe+2} for *L. ferriphilum*, q_{EPS} and q_{Fe+2} for *F. acidiphilum*) to a maximum value of 10 (mmol/GDW/h). The optimal value of the objective function for each deletion or "mutant" was evaluated and compared with the "wild-type" value to determine the effect of the enzyme deletion on the optimal growth rate. The ratio between the objective function with the enzyme deletion (Z_{mut}) and the wild-type (Z_{wt}) were calculated and plotted as shown in Figures 3 and 4 for *L. ferriphilum* and *F. acidiphilum*.

The knockout simulations were made in order to determine the model predictions based on the effect of the elimination of different enzymes involved in central metabolism. The deletion of enzymes that cause no growth were classified as essential enzymes, and were compared with literature information about key enzymes to check the consistency. The experimental knockouts could not be developed because of the impossibility to transform this type of microorganisms.

According to Figure 3, the action of enzymes PEPS, ENO, and PGM, which participate in the Embden-Meyerhof-Parnas pathway, are essential for cell growth. PEPS catalyzes the anabolic conversion of pyruvate to phosphoenolpyruvate, and therefore defines the anabolic characteristic of the pathway, allowing the generation of glucose from CO_2. ENO and PGM catalyze the formation from phosphoenolpyruvate of glyceraldehyde 3-phosphate, which is an important intermediate that participates in the pentose phosphate pathway and lipid generation.

Under the conditions studied, all the enzymes of the reductive TCA cycle (FUM, MDH, FDR, SUC, OGOR, IDH, ACO, CCS, CCL, POR) are found to be necessary for growth, because this pathway is the only way for *L. ferriphilum* to fix CO_2. Experimentally, four enzymes of this cycle are described to be essential and make possible the reverse behavior of this cycle: FDR, OGOR, CCS, CCL, and POR.[19,38,39]

From the pentose phosphate pathway, only the deletion of RPI was found to be lethal for cell growth. This enzyme is the only source of formation of D-Ribose 5-phosphate, which is a precursor of 5-phosphoribosyl-1-pyrophosphate (prpp) from which nucleotides and several amino acids are formed.

Respiration enzymes were symbolized by REDCYT as the ferrous oxidizer, CYTcbb3 as the electron transporter from ferrous iron to O_2, and NDH for the formation of reductive power by the reverse electron transfer from ferrous iron to NDH ubiquinone. These three enzymes, as well as ATP synthetase, are indispensable for growth, because ferrous iron is the only source of energy and reducing power of this bacterium, and the exchange of protons derived from this process, executed by ATP synthetase, is the main source of ATP for the cell.

The other enzymes studied correspond to those that catalize anaplerotic reactions PC and PEPC. Deletion of one of these does not affect cell growth since the anapletoric function is carried out by the other one. The rest are enzymes that catalyze reactions in the pentose phosphate pathway, whose removal results in a smaller growth rate, indicating that other reactions could compensate their knockout.

Several differences between microorganisms appear when the results of the previous analysis are compared. For *F. acidiphilum* more enzymes of glycolysis are necessary for growth, like GAP, PGK, ENO, PGM, PYK, and PFK

because this pathway is its only way to obtain energy from organic carbon sources. Of these enzymes, PFK and PYK have been described as key enzymes of this pathway.[37] Moreover, respiration enzymes for reductive power and ATP generation (NDH and ATP) appear to be essential; however, the knockout of enzymes involved in ferrous iron oxidation (symbolized by BLUECYT for iron oxidation and UBIQ for electron transport) results in a slight decrease in cell growth of about 6%, due to the chemoorganotrophic capacities of this microorganism, allowing it to obtain energy from organic carbon metabolism by glycolysis.

It is also observed that almost all TCA cycle enzymes are essential except SUC, because there is an alternative reaction to generate succinate from lysine synthesis from aspartate, which compensates the knockout of SUC, thus supporting cell growth. If both reactions are deleted, growth is not possible for this archaea.

From this analysis, it is possible to observe that the growth predictions restricted to enzyme deletions are consistent with literature information about the key enzymes for growth in central metabolism of both microorganisms, showing a good performance of the metabolic models.

CONCLUSIONS

A metabolic model for a mixed culture composed by *L. ferriphilum* and *F. acidiphilum* was reconstructed from literature and data base information. With this model and a FBA methodology, the biomass yields for both populations growing on ferrous iron were estimated, obtaining very reasonable values. The metabolic model of *L. ferriphilum* was developed based on a stoichiometric model of a similar species, *L. ferrooxidans,* The previous model was modified considering the specific metabolic differences between these species as described in the literature.

Specific features of *F. acidiphilum* metabolism were included in the metabolic model taken from the literature, for instance the chemomixotrophic capacity of this archaea to grow on ferrous iron and also organic carbon as energy sources. Specifically, it was simulated that *F. acidiphilum* can use the EPS secreted by *L. ferriphilum*, and ferrous iron from culture media for growth.

Cell growth of *F. acidiphilum* on different substrates was also tested, obtaining specific growth rates for each one. With this methodology, it is possible to obtain a clear notion about useful substrates that could maximize cell growth, and then design and suggest an appropriate composition of the culture media.

From knockout enzyme simulations it was possible to check the essential enzymes for growth, and therefore, predict which enzymes could be removed without affecting (or only slightly affecting) cell growth. From this analysis, most of the key enzymes predicted were consistent with literature information, indicating a good performance of both metabolic models.

This work describes the first metabolic model available for a mixed culture of *L. ferriphilum* and *F. acidiphilum*. This first approach allowed obtention of a deeper understanding of the metabolism of these microorganisms growing together, such as their main interactions and metabolite exchange.

With the information obtained from these analyses it could be possible to predict which specie will be dominant under defined conditions, and thus estimate the percentage of each one in the culture at steady state. Further experimental work will be necessary for this purpose and to fully address the predictive capacity of the model. More extensive studies of these microorganisms growing alone and together are required to evaluate the predicted values and determine the composition of the culture media which enables the maximum growth rate of both species, and therefore provide new strategies to enhance and optimize productivity in bioleaching processes.

NOTATION

S = Stoichiometric matrix
$v(x)$ = Vector of intracellular reaction rates
b = Vector of extracellular reaction rates (substrate consumption and products formation) (mol/GDW·h)
Y_{CX} = Growth yield in carbon (GDW/C-mol)
Y_{FeX} = Growth yield in ferrous iron (C-mol/mol Fe^{+2})
q_{CO2} = Specific consumption rate of CO_2 (C-mol/GDW·h)
q_{EPS} = Specific production rate of exopolysaccharides by *L. ferriphilum* (mol EPS/GDW·h)
q_{Fe+2} = Specific consumprion rate of ferrous iron (mol Fe^{+2}/GDW·h)
μ = Specific growth rate (1/h)
Z_{mut} = Objective function with enzyme deletion (1/h)
Z_{wt} = Objective function for wild-type strain (1/h)

Acknowledgments

The authors are gratefully acknowledge the Basal Programme of Conicyt for funding of the Centre for Biotechnology and Bioengineering, CeBiB (project FB0001) and Conicyt and BioSigma S.A. for support of M.P.M.

Literature Cited

1. Schippers A, Sand W. 1999. Bacterial leaching of metal sulfides proceeds by two indirect mechanisms via thiosulfate or via polysulfides and sulfur. *Appl Environ Microbiol*. 65:319–321.
2. Holmes DS, Bonnefoy V. 2007. Genetic and bioinformatics insights into iron and sulfur oxidation mechanisms of bioleaching organisms. In: Rawlings D, Johnson B, editors. Biomining. Berlin: Springer.
3. Baker BJ, Banfield JF. 2003. Microbial communities in acid mine drainage. *FEMS Microbiol Ecol*. 44:139–152.
4. Ram RJ, Verberkmoes NC, Thelen MP, Tyson GW, Baker BJ, Blake RC II, Shah M, Hettich RL, Banfield JF. 2005. Community proteomics of a natural microbial biofilm. *Science*. 308: 1915–1920.
5. Tyson GW, Chapman J, Hugenholtz P, Allen EE, Ram RJ, Richardson PM, Solovyev VV, Rubin EM, Rokhsar DS, Banfield JF. 2004. Community structure and metabolism through reconstruction of microbial genomes from the environment. *Nature*. 428:37–43.
6. Goltsman DS, Dasari M, Thomas BC, Shah MB, VerBerkmoes NC, Hettich RL, Banfield JF. 2013. New group in the *Leptospirillum* clade: cultivation-independent community genomics, proteomics and transcriptomics of the new species "*Leptospirillum* group IV UBA BS". *Appl Environ Microbiol*. 79:5384–5393.
7. Rawlings DE, Tributsch H, Hansford GS. 1999. Reasons why '*Leptospirillum*'-like species rather than *Thiobacillus*

ferrooxidans are the dominant iron-oxidizing bacteria in many commercial processes for the biooxidation of pyrite and related ores. *Microbiology*. 145 (Pt 1):5–13.
8. Mi S, Song J, Lin J, Che Y, Zheng H, Lin J. 2011. Complete genome of *Leptospirillum ferriphilum* ML-04 provides insight into its physiology and environmental adaptation. *J Microbiol*. 49:890–901.
9. Dopson M, Baker-Austin C, Hind A, Bowman JP, Bond PL. 2004. Characterization of *Ferroplasma* isolates and *Ferroplasma acidarmanus* sp. nov., extreme acidophiles from acid mine drainage and industrial bioleaching environments. *Appl Environ Microbiol*. 70:2079–2088.
10. Golyshina OV, Pivovarova TA, Karavaiko GI, Kondrateva TF, Moore ER, Abraham WR, Lunsdorf H, Timmis KN, Yakimov MM, Golyshin PN. 2000. *Ferroplasma acidiphilum* gen. nov., sp. nov., an acidophilic, autotrophic, ferrous-iron-oxidizing, cell-wall-lacking, mesophilic member of the Ferroplasmaceae fam. nov., comprising a distinct lineage of the Archaea. *Int J Syst Evol Microbiol*. 50 (Pt 3):997–1006.
11. Golyshina OV, Timmis KN. 2005. *Ferroplasma* and relatives, recently discovered cell wall-lacking archaea making a living in extremely acid, heavy metal-rich environments. *Environ Microbiol*. 7:1277–1288.
12. Pivovarova TA, Kondrat'eva TF, Batrakov SG, Esipov SE, Sheichenko VI, Bykova SA, Lysenko AM, Karavaiko GI. 2002. Phenotypic features of *Ferroplasma acidiphilum* strains Yt and Y-2. *Mikrobiologiia*. 71:809–818.
13. Yelton AP, Comolli LR, Justice NB, Castelle C, Denef VJ, Thomas BC, Banfield JF. 2013. Comparative genomics in acid mine drainage biofilm communities reveals metabolic and structural differentiation of co-occurring bacteria. *BMC Genomics*. 14:485.
14. Mahadevan R, Bond DR, Butler JE, Esteve-Nunez A, Coppi MV, Palsson BO, Schilling CH, Lovley DR. 2006. Characterization of metabolism in the Fe(III)-reducing organism *Geobacter sulfurreducens* by constraint-based modeling. *Appl Environ Microbiol*. 72:1558–1568.
15. Geng J, Song HS, Yuan J, Ramkrishna D. 2012. On enhancing productivity of bioethanol with multiple species. *Biotechnol Bioeng*. 109:1508–1517.
16. Zomorrodi AR, Maranas CD. 2012. OptCom: a multi-level optimization framework for the metabolic modeling and analysis of microbial communities. *PLoS Comput Biol*. 8: e1002363.
17. Hold C, Andrews BA, Asenjo JA. 2009. A stoichiometric model of *Acidithiobacillus ferrooxidans* ATCC 23270 for metabolic flux analysis. *Biotechnol Bioeng*. 102:1448–1459.
18. Merino MP, Andrews BA, Asenjo JA. 2010. Stoichiometric model and metabolic flux analysis for *Leptospirillum ferrooxidans*. *Biotechnol Bioeng*. 107:696–706.
19. Levican G, Ugalde JA, Ehrenfeld N, Maass A, Parada P. 2008. Comparative genomic analysis of carbon and nitrogen assimilation mechanisms in three indigenous bioleaching bacteria: predictions and validations. *BMC Genomics* 9:581.
20. Barreto M, Jedlicki E, Holmes DS. 2005. Identification of a gene cluster for the formation of extracellular polysaccharide precursors in the chemolithoautotroph *Acidithiobacillus ferrooxidans*. *Appl Environ Microbiol*. 71:2902–2909.
21. Dopson M, Baker-Austin C, Bond PL. 2005. Analysis of differential protein expression during growth states of *Ferroplasma* strains and insights into electron transport for iron oxidation. *Microbiology*. 151(Pt 12):4127–4137.
22. Nemoto N, Shida Y, Shimada H, Oshima T, Yamagishi A. 2003. Characterization of the precursor of tetraether lipid biosynthesis in the thermoacidophilic archaeon *Thermoplasma acidophilum*. *Extremophiles*. 7:235–243.
23. Batrakov SG, Pivovarova TA, Esipov SE, Sheichenko VI, Karavaiko GI. 2002. Beta-D-glucopyranosyl caldarchaetidylglycerol is the main lipid of the acidophilic, mesophilic, ferrous iron-oxidising archaeon *Ferroplasma acidiphilum*. *Biochim Biophys Acta*. 1581:29–35.
24. Nishihara M, Yamazaki T, Oshima T, Koga Y. 1999. sn-glycerol-1-phosphate-forming activities in Archaea: separation of archaeal phospholipid biosynthesis and glycerol catabolism by glycerophosphate enantiomers. *J Bacteriol*. 181:1330–1333.
25. Koga Y, Morii H. 2007. Biosynthesis of ether-type polar lipids in archaea and evolutionary considerations. *Microbiol Mol Biol Rev*. 71:97–120.
26. Pe'er I, Felder CE, Man O, Silman I, Sussman JL, Beckmann JS. 2004. Proteomic signatures: amino acid and oligopeptide compositions differentiate among phyla. *Proteins*. 54:20–40.
27. Stephanopoulos GN, Aristidou AA, Nielsen J. 1998. *Metabolic Engineering*. London: Academic Press.
28. Ingraham JL, Maaloe O, Neidhardt FC. 1983. *Growth of the bacterial cell*. Sunderland: Sinnauer Associates.
29. Feist AM, Scholten JC, Palsson BO, Brockman FJ, Ideker T. 2006. Modeling methanogenesis with a genome-scale metabolic reconstruction of *Methanosarcina barkeri*. *Mol Syst Biol*. 2: 2006.0004.
30. Varma A, Palsson BO. 1993. Metabolic capabilities of *Escherichia Coli*. I. Synthesis of biosynthetic precursors and cofactors. *J Theor Biol*. 165:477–502.
31. Gahan CS, Sundkvist JE, Dopson M, Sandstrom A. 2010. Effect of chloride on ferrous iron oxidation by a *Leptospirillum ferriphilum*-dominated chemostat culture. *Biotechnol Bioeng*. 106: 422–431.
32. Pardelha F, Alburquerque MG, Reis MA, Dias JM, Olivera R. 2012. Flux balance analysis of mixed microbial cultures: application to the production of polyhydroxyalkanoates from complex mixtures of volatile fatty acids. *J Biotechnol*. 162:336–345.
33. Llaneras F, Pico J. 2007. A procedure for the estimation over time of metabolic fluxes in scenarios where measurements are uncertain and/or insufficient. *BMC Bioinformatics*. 8:421.
34. Makarova KS, Aravind L, Galperin MY, Grishin NV, Tatusov RL, Wolf YI, Koonin EV. 1999. Comparative genomics of the Archaea (Euryarchaeota): evolution of conserved protein families, the stable core, and the variable shell. *Genome Res*. 9:608–928.
35. Selkov E, Maltsev N, Olsen GJ, Overbeek R, Whitman WB. 1997. A reconstruction of the metabolism of *Methanococcus jannaschii* from sequence data. *Gene*. 197:GC11–GC26.
36. She Q, Singh RK, Confalonieri F, Zivanovic Y, Allard G, Awayez MJ, Chan-Weiher CC-Y, Clausen IG, Curtis BA, De Moors A, Erauso G, Fletcher C, Gordon PMK, Heikamp-de Jong I, Jeffries AC, Kozera CJ, Medina N, Peng X, Thi-Ngoc HP, Redder P, Schenk ME, Theriault C, Tolstrup N, Charlebois RL, Doolittle WF, Duguet M, Gaasterland T, Garrett RA, Ragan MA, Sensen CW, Van der Oost J. 2001. The complete genome of the crenarchaeon *Sulfolobus solfataricus* P2. *Proc Natl Acad Sci U S A*. 98:7835–7840.
37. Verhees CH, Kengen SW, Tuininga JE, Schut GJ, Adams MW, De Vos WM, Van Der Oost J. 2003. The unique features of glycolytic pathways in Archaea. *Biochem J*. 375:231–246.
38. Campbell BJ, Cary SC. 2004. Abundance of reverse tricarboxylic acid cycle genes in free-living microorganisms at deep-sea hydrothermal vents. *Appl Environ Microbiol*. 70: 6282–6289.
39. Hugler M, Huber H, Stetter KO, Fuchs G. 2003. Autotrophic CO2 fixation pathways in archaea (*Crenarchaeota*). *Arch Microbiol*. 179:160–173.

APPENDIX 1

Reactions used in the stoichiometric model of *Ferroplasma acidiphilum*. Irreversible reactions are indicated with an arrow (=>), and reversible reactions with an equal (=)

	Glycolysis
A1	glc + atp => g6p + adp + h
A2	f6p = g6p
A3	2 * gap + h2o = f6p + p
A4	gap + nad + p + adp => g3p + atp + nadh + h
A5	pep + h2o = g3p
A6	pep + amp + p + 2 * h => pyr + atp + h2o
	Pentose Phosphate
A7	g6p + 2 * nad + h2o => ribu5p + 2 * nadh + co2 + 2 * h
A8	ribu5p = xyl5p
A9	ribu5p=rib5p
A10	xyl5p + rib5p = gap + sed7p
A11	ery4p + xyl5p = gap + f6p
A12	gap + sed7p = ery4p + f6p
	TCA cycle
A13	pyr + coa + nad => accoa + co2 + nadh
A14	h2o + oac + accoa => cit+ h + coa
A15	cit + nad => akg + nadh + co2
A16	akg + nad + coa = succoa + nadh + co2
A17	succoa + p + adp => suc + coa + atp
A18	suc + coq = fum + coqh2
A19	fum + h2o + nad => oac + nadh + h
	Anaplerotic Reaction
A20	pyr + co2 + atp + h2o => oac + adp + p + 2 * h
A21	pep + co2 + h2o => oac + p + h
	Oxidative Phosphorylation
A22	2 * ferrous + 0.5 * o2 + 2 * H_in => 2 * ferric + h2o
A23	nadh + coq +4 * H_in +h => coqh2 + nad + 4 * H_out
A24	3 * H_out + adp + p +h => 3 * H_in +atp + h2o
	Amino Acid Biosynthesis
A25	nh4 + akg + nadh + h => glut + nad + h2o
A26	nh4 + glut + atp => glum + adp + p
A27	glut + atp + 2 * nadh + h =>pro + adp + 2 * nad + p + h2o
A28	2 * atp + glum + co2 + 2 * h2o => glut + 2 * adp + p + carp + 3 * h
A29	2 * glut + accoa + aspt + 2 * atp + 2 * h2o + nadh + carp => argi + fum + amp + adp + coa + nad + acet + akg + 4 * p + 4 * h
A30	aspt + atp + 2 * nadh + 2 * h + pyr + succoa + glut =>lys + adp + 2 * nad + p + coa + akg + suc + co2
A31	oac + glut = aspt + akg
A32	aspt + atp + 2 * nadh + 2 * h => hser + p + 2 * nad + adp
A33	hser + succoa + cys + mythf + h2o =>met + coa + suc + pyr + nh4 + h + thf
A34	hser + atp + h2o => thr + adp + p + h
A35	thr + pyr + nadh + 2 * h + glut => ile + nh4 + co2 + nad + h2o + akg
A36	aspt + atp + nh4 + h2o => asn + 2 * p + amp + h
A37	2 * pep + ery4p + nadh + atp => chor + adp + nad + 4 * p
A38	chor + h + glut => phen + co2 + h2o + akg
A39	chor + nad + glut => tyr + akg + nadh + co2
A40	chor + glum + prpp + ser =>tryp + pyr + glut + 2 * p + h2o + co2 + gap + 2 * h
A41	2 * pyr + nadh + 2 * h => kiv + nad + co2 + h2o
A42	kiv + glut = val + akg
A43	kiv + h2o + accoa + nad + glut =>leu + coa + nadh + h + co2 + akg

Continued

A44	pyr + glut = ala + akg
A45	g3p + glut + nad + h2o => ser + akg + nadh + p + h
A46	ser + thf = gly + mthf + h2o
A47	ser + accoa + hs => cys + coa + acet
A48	rib5p + atp => prpp + amp + h
A49	prpp + 2 * glum + gly + 5 * atp + aspt + fthf + 4 * h2o + co2 => aicar + 5 * adp + 7 * p + 2 * glut + thf + fum + 9 * h
A50	prpp + glum + atp + 2 * nad + 5 * h2o => his + aicar + akg + 2 * nadh + 7 * h + 5 * p
	Nucleotide Biosynthesis
A51	aicar + fthf = thf + imp + h2o + 2 * h
A52	imp + aspt + atp => amp + adp + p + fum + h
A53	amp + nadh + h = damp + nad + h2o
A54	imp + nad + 2 * h2o + atp + nh4 => gmp + amp + nadh + 2 * p + 3 * h
A55	gmp + nadh + h => dgmp + nad + h2o
A56	carp + aspt + 1/2 * o2 + prpp => ump + h2o + co2 + 3 * p + h
A57	ump + 2 * atp + 2 * nadh + h2o + mthf => dtmp + 2 * adp + 2 * nad + 2 * p + thf
A58	ump + nh4 + atp = cmp + adp + p + h
A59	cmp + nadh + h => dcmp + nad + h2o
	Phospholipid Biosynthesis
A60	gap + nadh + 2 * h = glyc1p + nad
A61	3 * accoa+2 * nadh+3 * atp+h2o+h=>3 * coa+2 * nad+3 * adp+co2+p+ipp
A62	glyc1p + 8 * ipp + cmp + 2 * atp + 9 * h2o = cdparch + 2 * adp + 17 * h + 18 * p
A63	cdparch + glyc1p + h2o = archglyc + cmp + p + h
	Protein Biosynthesis
A64	0.078 * ala + 0.06 * argi + 0.034 * asn + 0.056 * aspt + 0.008 * cys + 0.074 * glut + 0.02 * glum + 0.076 * gly + 0.016 * his + 0.076 * ile + 0.096 * leu + 0.058 * lys + 0.025 * met + 0.038 * phen + 0.045 * pro + 0.06 * ser + 0.05 * thr + 0.01 * tryp + 0.082 * val + 0.038 * tyr + 4.3 * atp + 4.3 * h2o=>prot + 4.3 * adp + 4.3 * p + 4.3 * h
	DNA Biosynthesis
A65	0.65 * damp + 0.65 * dtmp + 0.35 * dcmp + 0.35 * dgmp + 6.8 * atp + 6.8 * h2o=>dna + 6.8 * adp + 6.8 * p + 6.8 * h
	RNA Biosynthesis
A66	0.175 * cmp + 0.175 * gmp + 0.325 * amp + 0.325 * ump + 2 * atp + 2 * h2o=>rna + 2 * adp + 2 * p + 2 * h
A67	2 * archglyc + glc => lipI + glyc1p
A68	2 * archglyc + 3 * glc => lipII + glyc1p
A69	0.55 * lipI + 0.35 * lipII=>lip
	Carbohydrate Biosynthesis
A70	g6p + atp + h2o=polys + adp + h
	Biomass Formation
A71	0.040 * dna + 0.24 * rna + 0.62 * prot + 0.01 * polys + 0.09 * lip =>bio

Manuscript received Jun. 12, 2014, and revision received Nov. 20, 2014.